Effect of Diffusion of Coal Pyrolysis Products on the Ignition Characteristics and Conditions of Coal–Water Fuel Droplets

G. V. Kuznetsov[a], V. V. Salomatov[b], and S. V. Syrodoi[a]

UDC 536.468

Abstract: This paper presents a theoretical study of the thermal preparation and ignition of a coal–water fuel droplet under intense radiative-convective heating with diffusion of gaseous pyrolysis products of the solid fuel into the ambient gaseous medium. It has been found that gaseous pyrolysis products are ignited at a distance from the heating surface approximately equal to the radius of the droplet, after which the coke of the main fuel layer is ignited. The time between the ignition of volatiles and the coke residue is less than 0.5 s. Comparison of the ignition delays obtained by mathematical modeling and experimentally has shown satisfactory agreement between theoretical and experimental values.

Keywords: coal–water fuel, coke ignition, ignition of volatile, diffusion of pyrolysis products.

DOI: 10.1134/S0010508218060047

INTRODUCTION

The economic viability of using coal–water fuel (CWF) as the main one for thermal power plants was proved long ago [1–3]. However, until now, the CWF technology has not been used widely in modern power engineering. This is due to the lack of a general theory of ignition and combustion of substantially heterogeneous fuels. The mathematical models and methods developed to date to solve ignition problems of CWF particles can be divided into three groups.

The first group includes zero-dimensional models [4–6], which assume that the temperature field of a fuel particle is uniform and the evaporation process is localized directly on its surface. Such models are the simplest and provide analytical expressions for calculating ignition characteristics. In this case, the hypothesis of localization of the evaporation front on the particle surface is an important assumption and can lead to large errors in predicting ignition conditions and characteristics.

The second group includes models [7–9] in which the CWF ignition process is divided into a series of successive stages corresponding to certain physical processes (inert heating, water evaporation, thermal decomposition of the organic part of the fuel, ignition). It is necessary to note that in practice, thermal preparation processes occur simultaneously for a long time. Accordingly, discretization of the ignition process into separate time stages can lead to significant errors in modeling the ignition of CWF droplets.

The third, most common, group of CWF ignition models is constructed on the basis of the equations of mathematical physics [10]. The ignition process is described by a system of unsteady partial differential equations taking into account [10] the main physical and chemical processes occurring during the induction period. However, at present, the mathematical apparatus of [10] has been used to investigate the effect of only a small group of significant factors (thermal radiation [11], particle shape [12], degree of coal metamorphism [13], the heterogeneity of the porous structure of the fuel [14]) on the CWF ignition conditions and characteristics. In formulations [10–14], it is assumed that volatile ignition proceeds in a very narrow (infinitely thin) near-surface film. However, it is known

[a]Tomsk Polytechnic University, Tomsk, 634050 Russia; ssyrodoy@yandex.ru.
[b]Kutateladze Institute of Thermophysics, Siberian Branch, Russian Academy of Sciences, Novosibirsk, 630090 Russia.

from [15] and [16] that diffusion processes play a significant and even decisive role in the ignition of solid fuels (e.g., coal). One of the most complete models for the ignition of a CWF droplet is given in [17]. It describes the evaporation of water and thermal decomposition of the organic part of the fuel, accompanied by the release of volatiles and their ignition in the gas phase. In [17], water evaporation is taken into using the Stefan conditions (equilibrium temperature and velocity at the evaporation front). However, the fact that the evaporation rate depends on the surface temperature of the phase transition front and the concentration of liquid vapor at this surface was found as early as in Hertz study [18].

Based on the above, we can conclude that the modeling of the ignition of substantially inhomogeneous CWF particles in describing the main interrelated physical processes of thermal preparation (including volatile diffusion) occurring both within a particle and in its small neighborhood in the induction period is an important problem that has not been solved so far.

This paper presents a mathematical modeling of heat and mass transfer processes occurring simultaneously during ignition of a CWF particle taking into account the diffusion of gaseous products of thermal decomposition into the ambient gas region.

1. FORMULATION OF THE PROBLEM

1.1. Physical Formulation of the Problem

The main regularities of the investigated process have been established in experimental studies [14]. The results of [14] were used to develop a physical model of heat and mass transfer processes under conditions of simultaneously occurring intense phase (evaporation of water) and physicochemical (thermal decomposition, release of volatiles, interaction of water vapor and coke carbon, gas-phase ignition of pyrolysis products) transformations corresponding to the conditions of experiments [14].

At the initial time, a CWF particle is introduced into a high-temperature medium and is heated by convection and radiation. Intense heating initiates water evaporation. The evaporation front moves away from the surface deep into the fuel. As a result, a porous coal matrix with high thermal resistance is formed. Water vapor generated by evaporation are filtered through the dry fuel layer and involved in thermochemical interaction with carbon to form flammable gaseous products (CO and H_2). Heating of a CWF particle leads to thermal decomposition and release of volatiles. The latter, together with water vapor and the products of their thermochemical interaction with carbon, are filtered to the surface of the fuel particle. After that, they diffuse into the ambient gaseous medium. As a result, a vapor–gas mixture with a significant gradient of concentrations of pyrolysis products is formed. When the temperature and mass ratio of volatiles and oxidizer reach critical values, ignition occurs. Intense heating by the flame of volatiles initiates combustion of the CWF coke.

It should be noted that thermal decomposition produces a gas mixture whose chemical composition significantly depends on a number of factors, such as the degree of metamorphism of coal, moisture, and deposit.

1.2. Mathematical Formulation of the Problem

The mathematical formulation of the problem of CWF ignition corresponding to the physical model formulated above includes a system of unsteady differential equations.

The solution domain of the problem (CWF particle–gas medium) is given in Fig. 1. Intense heating initiates evaporation of water and leads to the formation of a substantially heterogeneous structure consisting of solid, liquid, and gaseous components. The temperature distribution in this heterogeneous system is described by an energy equation [10] that takes into account water evaporation, thermal decomposition of the organic part of the fuel, the thermochemical interaction between water vapor and carbon, and the movement of water vapor and thermal decomposition products through the porous matrix:

$$\frac{\partial H}{\partial t} = \frac{1}{r^2}\frac{\partial}{\partial r}\left[r^2 \lambda_{\text{CWF}} \frac{\partial T}{\partial r}\right] - \frac{Q_{\text{eva}}W_{\text{eva}}}{h_d}\delta(r_{\text{eva}})$$

$$- \sum_{i=1}^{i=2} Q_i W_i - c_s \rho_s U_s \frac{\partial T}{\partial r}\theta(r - r_{\text{eva}}), \qquad (1)$$

$$t > 0, \quad 0 < r < r_{\text{out}}.$$

Here

$$\sum_{i=1}^{n=2} Q_i W_i = Q_{\text{c}\rightarrow\text{vol}}W_{\text{c}\rightarrow\text{vol}} + Q_{\text{C}+\text{H}_2\text{O}}W_{\text{C}+\text{H}_2\text{O}},$$

$H = c_{\text{CWF}}(r)\rho_{\text{CWF}}(r)T(r,\tau)$ is the enthalpy, r is the radius of the particle (r_{out} is the outer radius), $\delta(r_{\text{eva}})$ is the Dirac function, $\theta(r_{\text{eva}})$ is the Heaviside function, h_d is the spread parameter of the evaporation front [19], T is the temperature, λ_{CWF} is the thermal conductivity of the fuel [in W/(m·K)], c_{CWF} is the specific heat of the fuel (in J/kg), and ρ_{CWF} is the density of the fuel (in kg/m^3), U_s is the filtration rate of water vapor and gaseous products of thermal decomposition (in m/s), c_s and ρ_s are the heat capacity and density of the mixture of water vapor and gaseous pyrolysis products, Q and W are the heat effect and the flow rate
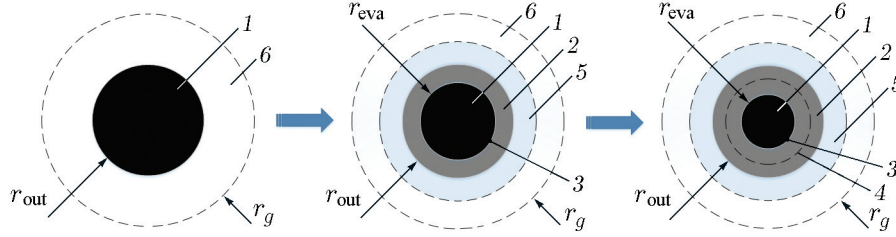
Fig. 1. Schematic of the solution domain: (1) initial fuel; (2) dry coal matrix; (3) interface between the initial fuel and the dry coal matrix; (4) interface between the dry coal matrix and thermally decomposing coal; (5) vapor–gas mixture; (6) ambient gas region.

of the corresponding process (the subscript eva refers to water evaporation, $c \to vol$ to thermal decomposition, and $C + H_2O$ to thermochemical interaction of carbon and water vapor). Thermophysical characteristics λ_{CWF}, c_{CWF}, and ρ_{CWF} were specified taking into account the position of the phase-transition boundary. The mass evaporation rate was calculated from the expression [20]

$$W_{eva} = W_f \exp\left[\frac{Q_{wat}\mu(T(r_{eva},\tau) - T_f)}{RT_f T(r_{eva},\tau)}\right] \ [kg/(m^2 \cdot s)], \quad (2)$$

where μ [kg/mol] is the molar mass of water and R [J/(mol·K)] is the universal gas constant; the subscript "wat" denotes parameters related to water. The coordinate of the evaporation boundary was found from the expression

$$r_{eva} = r_{out} - \int_0^t u_{fe}dt, \quad (3)$$

where $u_{fe} = W_{eva}/\rho$ [m/s] is the linear velocity of the evaporation front.

The temperature distribution in the gas region is described by an energy equation which takes into account the exothermic effects of oxidation reactions of the main combustible components:

$$c_g\rho_g\frac{\partial T}{\partial t} = \frac{\lambda_g}{r^2}\frac{\partial}{\partial r}\left[r^2\frac{\partial T}{\partial r}\right] + \sum_{i=1}^{n=4} Q_i W_i, \quad (4)$$

$$r_{out} < r < r_g.$$

Here

$$\sum_{i=1}^{n=4} Q_i W_i = Q_{CH_4+O_2}W_{CH_4+O_2}$$

$$+ Q_{CO+O_2}W_{CO+O_2} + Q_{H_2+O_2}W_{H_2+O_2}$$

$$- Q_{N_2+O_2}W_{N_2+O_2}$$

(Q_i and W_i are the heat effect and the rate of oxidation of the gas mixture components). At the CWF particle–gas interface, the conditions are specified by analogy

with [21, 22] taking into account the exothermic effect of the reaction of carbon with air oxygen $Q_{C+O_2}W_{C+O_2}$ and the thermal radiation from the ambient medium:

$$\frac{\partial T}{\partial r} = K_\lambda\frac{\partial T}{\partial r} + \frac{\varepsilon\sigma(T|_{r=r_g}^4 - T|_{r=r_{out}}^4)}{\lambda_{CWF}}$$

$$+ \frac{Q_{C+O_2}W_{C+O_2}}{\lambda_{CWF}}, \quad (5)$$

$$T(r_{out},t)|_{r=r-0} = T(r_{out},t)|_{r=r+0}.$$

Here $K_\lambda = \lambda_g/\lambda_{CWF}$, ε is the integral emissivity factor, and σ is the Stefan–Boltzmann constant. The rate of the reaction $C + O_2 = CO_2 + 18.67$ MJ/kg was calculated using the mathematical expression of the Arrhenius law:

$$W_i = k_{C+O_2}\left(1 - \sum_{i=1}^n C_i(r_{out},t) - C_{H_2O}(r_{out},t)\right)$$

$$\times \rho_g \exp\left(-\frac{E_{C+O_2}}{RT}\right). \quad (6)$$

Here k [m/s] is the pre-exponential factor, E [J/(mol·K)] is the activation energy of the chemical reaction, and C_i is the concentration of the ith component. It is assumed that water vapor moves together with the products of thermal decomposition through the porous coal matrix. The pressure distribution along the particle radius was determined from the piezoconductivity equation:

$$\frac{\partial p}{\partial t} = \frac{\chi}{r^2}\frac{\partial}{\partial r}\left(r^2\frac{\partial p}{\partial r}\right) + \frac{1}{m\rho Z}\sum_{i=1}^{n=2} f_i, \quad (7)$$

$$t > 0, \ 0 < r < r_{out}, \ p \geqslant p_g.$$

Here

$$\sum_{i=1}^{n=2} f_i = \frac{1}{s}(W_{c\to vol} + W_{C+H_2O \to CO+H_2}),$$

s [m] is the characteristic pore size, p [Pa] is the pressure, f_i is a function that determines the change in mass flow rate of the vapor–gas mixture as a result of

volatile release and absorption of water vapors during their thermochemical interaction with carbon, χ [m^2/s] is the piezoconductivity, Z [1/Pa] is the compressibility of water vapor, and m is the fuel porosity. The vapor filtration rate was determined from the differential expression of the Darcy law:

$$U_s = -\frac{K_p}{\nu}\frac{\partial p}{\partial r}. \tag{8}$$

Here ν [Pa$\cdot$s] is the dynamic viscosity and K_p [m^2] is the permeability of the medium. In the formulation of the problem, it is assumed that water vapor reacts endothermically with coal. The rate of the reaction $C + H_2O = CO + H_2 - 118.485$ MJ/kg was calculated by the formula

$$W_{C+H_2O} = k_{C+H_2O}c_{H_2O}\rho_s \exp\left(-\frac{E_{C+H_2O}}{RT}\right). \tag{9}$$

When $T_{surf} \geqslant T_{std}$ on the particle surface, the organic part of the fuel begins to decompose with the release of volatiles (T_{surf} is the surface temperature of the fuel particle and T_{std} is the temperature of onset of thermal decomposition). Thermal decomposition is described by the chemical kinetics equation

$$\frac{\partial \eta}{\partial t} = [1 - \eta]k_{c\to vol}\exp\left(-\frac{E_{c\to vol}}{RT}\right), \tag{10}$$
$$t > 0, \quad 0 < r < r_{out},$$

where η is the degree of pyrolysis of the fuel. The rate of pyrolysis was calculated by the expression

$$W = V_0[1 - \eta]k_{c\to vol}\rho_{CWF}\exp\left(-\frac{E_{c\to vol}}{RT}\right). \tag{11}$$

In the formulation of the problem, it was taken into account that the gaseous products of thermal destruction and chemical interaction of the solid residue of pyrolysis of coal and water vapor are injected into the near-wall region, thus forming a gas mixture which is ignited upon reaching critical values of the temperature and fuel concentration. The time period from the beginning of heating of the particle before the beginning of intense chemical reaction of the vapor–gas mixture with the oxidizer (the appearance of a local extremum on the temperature curve) is the ignition delay, according to the definition of [15]. The ignition criterion from [15] was used. In close proximity to the particle surface, the following reactions were taken into account:

(1) $H_2 + 0.5O_2 = H_2O + 141.900$ MJ/kg;

(2) $CO + 0.5O_2 = CO_2 + 100.90$ MJ/kg;

(3) $CH_4 + O_2 = CO_2 + H_2O + 55.00$ MJ/kg;

(4) $N_2 + O_2 = 2NO - 2\,987$ MJ/kg.

The rate of these reactions was calculated using the Arrhenius law:

$$W_i = k_i\left(1 - \sum_{i=1}^{n}C_i - C_{H_2O}\right)C_i\rho_g \exp\left(-\frac{E_i}{RT}\right). \tag{12}$$

The concentration of combustible components (H$_2$, CO, N$_2$, and CH$_4$) in a wall region of small thickness was calculated by solving the diffusion equation for the corresponding component:

$$\rho_g\frac{\partial C_i}{\partial t} = \frac{D_i\rho_g}{r^2}\frac{\partial}{\partial r}\left[r^2\frac{\partial C_i}{\partial r}\right] - W_i, \tag{13}$$
$$t > 0, \quad r_{out} < r < r_g.$$

Here D [m^2/s] is the diffusion coefficient. The concentrations of water vapor and carbon dioxide released during thermal decomposition were determined similarly:

$$\rho_g\frac{\partial C_i}{\partial t} = \frac{D_i\rho_g}{r^2}\frac{\partial}{\partial r}\left[r^2\frac{\partial C_i}{\partial r}\right], \tag{14}$$
$$t > 0, \ r_{out} < r < r_g.$$

System (1)–(14) was solved under the following boundary conditions:

$$t = 0 \to \begin{cases} T(r,t) = T_0 = 298 \text{ K}, \quad p(r,t) = p_g, \\ \qquad\qquad \eta(r,t) = 0; \quad 0 < r < r_g, \\ T(r,t) = T_g, \quad p(r,t) = p_g, \\ \qquad\qquad c_i(r,t) = 0; \quad r_{out} < r < r_g, \end{cases}$$

$$\left.\frac{\partial T}{\partial r}\right|_{r=0} = 0, \tag{15}$$

$$\left.\frac{\partial^2 T_g}{\partial r^2}\right|_{r=r_g} = 0, \tag{16}$$

$$\left.\frac{\partial p}{\partial r}\right|_{r=r_{eva}} = -\frac{\nu}{K_p}U_s(r_{eva}, t), \tag{17}$$

$$p(r_{out}, t) = p_g, \tag{18}$$

$$\left.\frac{\partial C_i}{\partial r}\right|_{r=r_{out}} = \frac{W_i}{\rho_g D_i}, \tag{19}$$

$$\left.\frac{\partial c_s}{\partial r}\right|_{r=r_{out}} = \frac{W_{eva}}{\rho_g D_s}, \tag{20}$$

$$\left.\frac{\partial^2 c_s}{\partial r^2}\right|_{r=r_g} = \left.\frac{\partial^2 c_i}{\partial r^2}\right|_{r=r_g} = 0 \tag{21}$$

(p_{atm} is the pressure of the ambient medium).

The thermal conductivity, heat capacity, and density of the wet and dehydrated parts of the CWF were calculated taking into account the volume fractions φ of the components:

$$\lambda_{\mathrm{CWF}} = \begin{cases} \lambda_1, & r \leqslant r_{\mathrm{eva}}, \\ \lambda_2, & r > r_{\mathrm{eva}}, \end{cases}$$

$$c_{\mathrm{CWF}} = \begin{cases} c_1, & r \leqslant r_{\mathrm{eva}}, \\ c_2, & r > r_{\mathrm{eva}}, \end{cases}$$

$$\rho_{\mathrm{CWF}} = \begin{cases} \rho_1, & r \leqslant r_{\mathrm{eva}}, \\ \rho_2, & r > r_{\mathrm{eva}}, \end{cases}$$

$$\lambda_1 = \varphi_3\lambda_3 + \varphi_4\lambda_4, \quad \lambda_2 = \varphi_3\lambda_3 + \varphi_5\lambda_5, \quad (22)$$

$$c_1 = \varphi_3 c_3 + \varphi_4 c_4, \quad c_2 = \varphi_3 c_3 + \varphi_5 c_5, \quad (23)$$

$$\rho_1 = \varphi_3\rho_3 + \varphi_4\rho_4, \quad \rho_2 = \varphi_3\rho_3 + \varphi_5\rho_5'; \quad (24)$$

the subscript 1 refers to the initial water-saturated fuel, 2 to the dry coal matrix, 3 to coal, 4 to water, and 5 to water vapor.

1.3. Baseline Data

The thermophysical properties of the initial fuel components (coal, water, and water vapor) used in the mathematical modeling are given in Table. 1. The composition of fuel volatile components are presented in Table 2, and thermochemical reaction constants in Table 3. Numerical studies were performed for the following initial data: $T_0 = 298$ K, $p_{\mathrm{atm}} = 101\,325$ Pa, and $\eta_0 = 0$. The molar mass of water was $\mu = 0.018$ kg/mol, and the permeability of coal was $K_p = 10^{-11}$ m^2.

1.4. Method for Solving Equations

The formulated problem of mathematical physics was solved by a finite difference method [31, 32]. The equations were approximated using an implicit four-point difference template [33]. For example, Eq. (1) was approximated as follows:

$$\frac{\partial H}{\partial t} = \frac{1}{r^2}\frac{\partial}{\partial r}\left[r^2\lambda_{\mathrm{CWF}}\frac{\partial T_1}{\partial r}\right] - \frac{Q_{\mathrm{eva}}W_{\mathrm{eva}}}{h_d}\delta(r_{\mathrm{eva}})$$

$$- \sum_{i=1}^{i=2}Q_iW_i - c_s\rho_s U_s\theta(r - r_{\mathrm{eva}})\frac{\partial T}{\partial r}$$

$$\rightarrow \frac{H_i^{n+1} - H_i^n}{\tau}$$

$$= \frac{1}{r_i^2}\frac{1}{h^2}\left[r_{i+0.5}^2\lambda_{i+0.5}(T_{i+1}^{n+1} - T_i^{n+1})\right.$$

$$\left. + r_{i-0.5}^2\lambda_{i-0.5}(T_i^{n+1} - T_{i-1}^{n+1})\right]$$

$$- \frac{Q_{\mathrm{eva}}W_{\mathrm{eva}}}{h}\delta(r_{\mathrm{eva}}) - \sum_{i=1}^{i=2}Q_iW_i$$

$$- c_s\rho_s U_s\theta(r - r_{\mathrm{eva}})\frac{T_{i+1}^{n+1} - T_{i-1}^{n+1}}{2h} \quad (i = 1, \ldots, N).$$
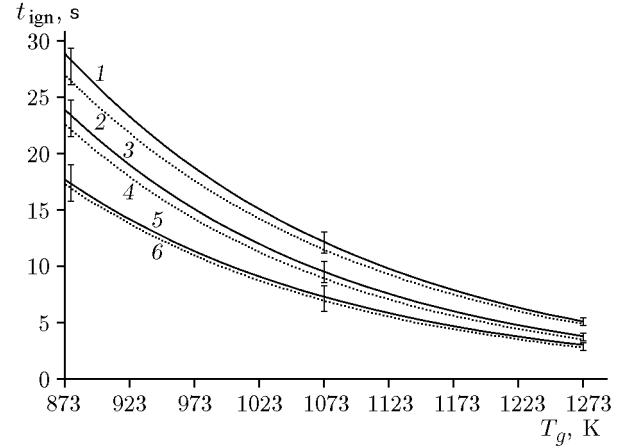

Fig. 2. Ignition delay of particles of a coal–water fuel based on D coal with different WCF particle diameter: $d = 3\cdot10^{-3}$ m (*1* and *2*), $2.5\cdot10^{-3}$ (*3* and *4*), and $2\cdot10^{-3}$ m (*5* and *6*); curves *1*, *3*, and *5* refer to the experimental data [14] and curves *2*, *4*, and *6* refer to the numerical solution.

Here $r_{i+0.5} = 0.5(r_i + r_{i+1})$ and $r_{i-0.5} = 0.5(r_i + r_{i-1})$. Similarly as for λ: $\lambda_{i+0.5} = 0.5(\lambda_i + \lambda_{i+1})$ and $\lambda_{i-0.5} = 0.5(\lambda_i + \lambda_{i-1})$.

The equations and boundary conditions (2)–(21) were approximated by a similar scheme. System (1)–(21) was solved in the period of time before the establishment of conditions adequate to the ignition conditions of solid, liquid, and heterogeneous fuels [15]. It should be noted that the calculations of fuel ignition in the presence of intense phase transformations (in particular, evaporation) are among the most difficult in combustion theory. This is due to the fact that water evaporation occurs in a very narrow (much smaller than the linear size of the particle) region (evaporation front). In this case, as a rule, the thermal effects of phase transitions are very high (up to $2.5\cdot10^6$ J/kg). As a result, an internal local heat sink occurs in the wet particle. The numerical study is complicated by the fact that the asymptotics of the evaporation and ignition processes are significantly different (ignition is a fast process, and evaporation is much slower). For this reason, a special algorithm based on the implicit separation of the phase transition front has been developed [34] to solve the formulated ignition problem.

2. RESULTS AND DISCUSSION

Figure 2 shows the results of a comparative analysis of the ignition delay t_{ign} of CWF droplets based on long-flame D coal obtained numerically [solution of

Table 1. Thermophysical Characteristics of the Main Fuel Components

Fuel component	λ, W/(m·K)	c_p, J/(kg·K)	ρ, kg/m³	Brown coal
D coal	0.206	1380	614	[23]
Brown coal	0.103	1150	700	[23]
Water	0.56	4190	1000	[24]
Water vapor	0.025	2038	0.58	[24]

Table 2. Composition of Gaseous Pyrolysis Products [25]

Component	Content of component, %	
	brown coal	hard coal
CO_2	15.5	2.3
CO	15.0	5.7
CH_4	20.5	65.9
H_2	25.6	18.6
N_2	23.4	7.5

Table 3. Thermochemical Reaction Constants

Reaction	Activation energy E_i, J/mol	Pre-exponential factor k_i, s⁻¹	Reference
Thermal decomposition c → vol	$39.4 \cdot 10^3$	178	[26]
$C + O_2 = CO_2$	$124.8 \cdot 10^3$	$6.4 \cdot 10^4$	[26]
$C + H_2O = CO + H_2$	$220 \cdot 10^3$	$2.07 \cdot 10^7$	[27]
$CO + 0.5O_2 = CO_2$	$200.0 \cdot 10^3$	$2.50 \cdot 10^{12}$	[28]
$H_2 + 0.5O_2 = H_2O$	$105.0 \cdot 10^3$	$1.13 \cdot 10^{17}$	[29]
$CH_4 + O_2 = CO_2$	$35 \cdot 10^3$	$5.1 \cdot 10^{14}$	[30]

system (1)–(21)] and experimentally [14]. It can be said that they are in satisfactory agreement (within a $\pm 17\%$ confidence interval of experimental data) in a fairly wide range of ambient temperatures ($800 < T_g < 1300$ K). Analysis of the dependences $t_{\text{ign}}(T_g)$ shows that the largest differences between the experimental and numerically calculated values of t_{ign} are observed at ambient temperature less than 970 K.

Curves of the ignition delay of a particle of a CWF based on brown coal (grade B) versus ambient temperature are presented in Fig. 3. Analysis of Figs. 2 and 3 shows that combustion of droplets of the CWF based on brown coal begins much earlier than combustion of the CWF based on D coal. This is primarily due to the higher volatile content in B coal compared to the long-flame coal. In general, the obtained numerical and experimental [14] ignition delays are in satisfactory agreement with each other.

Figure 4 illustrates the dynamics of the surface temperature (T_{surf}) of a CWF droplet. The entire period of thermal preparation can be divided into a number of successive characteristic stages. In the initial period of time (before $t \approx 0.18 t_{\text{ign}}$), there is inert heating of the fuel droplet (temperature grows slowly). After that, intense water evaporation is initiated. As a result, a porous coal matrix with low thermal conductivity and heat capacity is formed. It can be noted that the period of water evaporation is the longest. This is obviously due to the high endothermic effect of the phase transition (up to 2.5 MJ/kg), which causes a slowdown in the growth rate of T_{surf}. The characteristic break of the curve $T_{\text{surf}}(t)$ in Fig. 4 at the time $t \approx 0.7 t_{\text{ign}}$ corresponds to the ignition of volatiles. Intense heating from their flame causes initiation of combustion of the coke residue. This leads to a sharp change in the growth rate of T_{surf}.
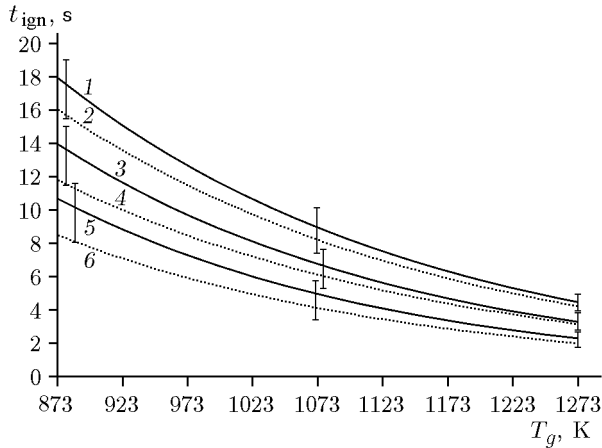
Fig. 3. Ignition delay of particles of a coal–water fuel based on B coal with different CWF particle diameter: $d = 3 \cdot 10^{-3}$ (*1* and *2*), $2.5 \cdot 10^{-3}$ (*3* and *4*), and $2 \cdot 10^{-3}$ m (*5* and *6*); curves *1*, *3*, and *5* refer to the experimental data [14] and curves *2*, *4*, and *6* refer to the numerical solution.

Fig. 5. Temperature distribution in the coal–water particle–gas system at the time of volatile ignition for $d = 2 \cdot 10^{-3}$ (*1*), $2.5 \cdot 10^{-3}$ (*2*), and $3 \cdot 10^{-3}$ m (*3*); EF is the temperature of the evaporation front.
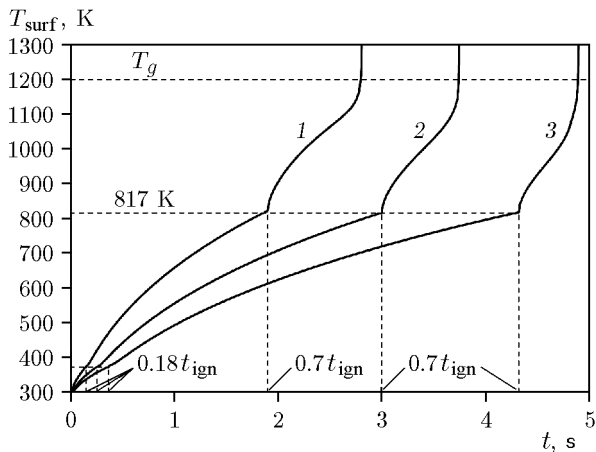

Fig. 4. Dynamics of the surface temperature of a coal–water fuel particle during heating at an ambient temperature $T_g = 1200$ K and $d = 2 \cdot 10^{-3}$ (*1*), $2.5 \cdot 10^{-3}$ (*2*), and $3 \cdot 10^{-3}$ m (*3*).

It may be noted that the dependence $T_{\text{surf}}(t)$ becomes exponential $\left(\dfrac{\partial T}{\partial t} \approx \exp\left[-\dfrac{E}{RT_{\text{surf}}} \right] \right)$.

Figure 5 shows the distributions of the dimensionless temperature in the water particle–gas system at the time of volatile ignition. It is seen that the initiation of combustion of gaseous pyrolysis products begins at some distance (approximately half the diameter of the CWF droplet) from the particle surface. This suggests that the diffusion of volatiles into the outer gas region and the formation of an extended and nonuniform con-
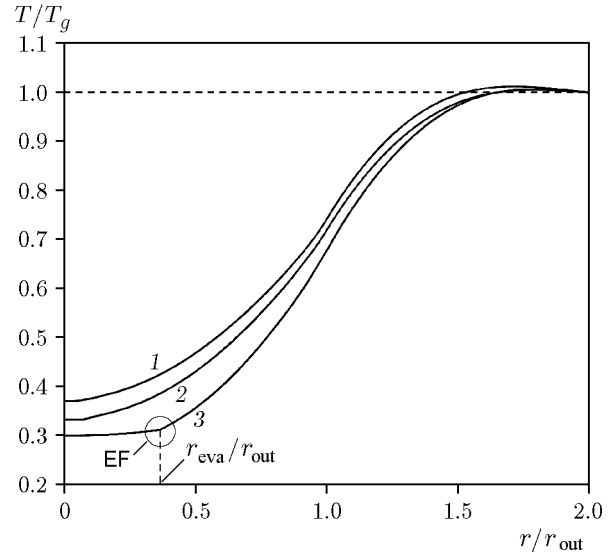
centration field play a significant role in the ignition of CWF droplets. It can be said that the use of the method of an infinitely thin reduced film in CWF ignition zones should be specifically justified when solving CWF ignition problems.

Analysis of the curves in Fig. 5 also shows that ignition of water-saturated CWF droplets is possible. Obviously, the combustion dynamics of CWF particles under conditions of continuing water evaporation will be significantly different from the oxidation of dry coal.

Figure 6 shows the ignition delay of CWF particles calculated for models [10] and (1)–(21). It can be noted that the values of t_{ign} obtained for model [10] are less than t_{ign} obtained by numerical solution of system (1)–(21). This is due to the fact that in [10–12], the diffusion of pyrolysis products into the ambient gaseous medium was not taken into account.

An analysis of the literature showed the absence of experimental data on the ignition delay of the coke residue. For this reason, predictive modeling of the carbon initiation process was performed. The results for D coal coke are presented in Fig. 7. Analysis of the dependences $t_{\text{ign}}(T_g)$ shows that coke starts to burn almost immediately after the ignition of volatiles. The interval between the times of ignition of volatiles and coke does not exceed 0.5 s.

Figure 8 shows the temperature distributions in the water-coal particle–gas system at the time of ignition of the coke residue. The temperature difference at the center of the CWF particle and on the surface is about
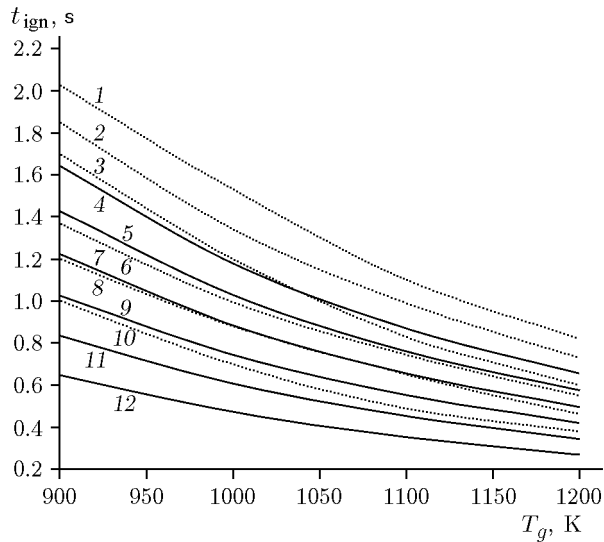
t_{ign}, s

Fig. 6. Ignition delay of particles of the coal–water fuel based on D coal versus ambient temperature calculated within the framework of different problem formulations: curves *1–3, 6, 8,* and *10* correspond to system (1)–(21) and curves *4, 5, 7, 9, 11,* and *12* to model [10]; curves *1* and *4* refer to $d = 0.9 \cdot 10^{-3}$ m, *2* and *5* to $d = 0.8 \cdot 10^{-3}$ m, *3* and *7* to $d = 0.7 \cdot 10^{-3}$ m, *6* and *9* to $d = 0.6 \cdot 10^{-3}$ m, *8* and *11* to $d = 0.5 \cdot 10^{-3}$ m, and *10* and *12* to $d = 0.4 \cdot 10^{-3}$ m.
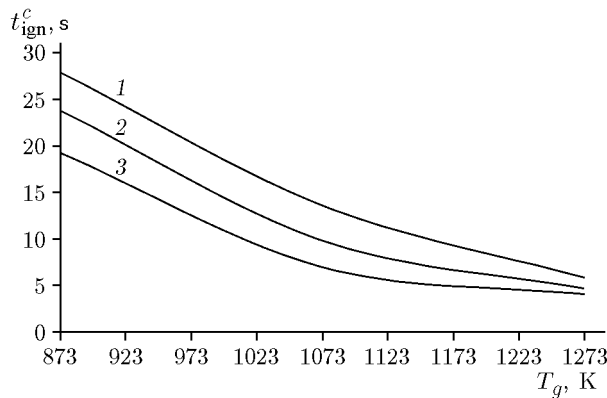
t_{ign}^{c}, s

Fig. 7. Ignition delay of the coke residue versus ambient temperature: curve *1* refers to $d = 3 \cdot 10^{-3}$ m, *2* to $d = 2.5 \cdot 10^{-3}$ m, and *3* to $d = 2 \cdot 10^{-3}$ m.

600 K. It can be said that the coke residue is ignited after the heating of the main fuel layer above the temperature of vapor formation. Note also that the temperature gradient is high. Accordingly, it can be reasonably assumed that ignition can give rise to thermal stresses in the particle structure, resulting in dispersion of the coal matrix.
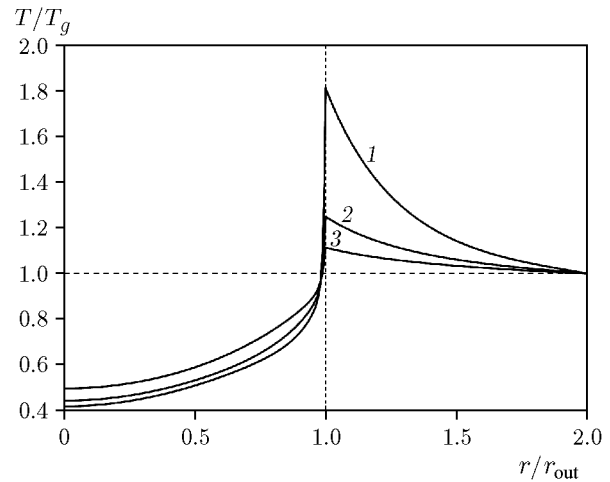
T/T_g

Fig. 8. Temperature distribution in the coal–water particle–gas system at the time of coke ignition at ambient temperature $T_g = 1200$ K: curve *1* refers to $d = 2 \cdot 10^{-3}$ m, *2* to $d = 2{,}5 \cdot 10^{-3}$ m, and *3* to $d = 3 \cdot 10^{-3}$ m.

CONCLUSIONS

A mathematical model of the thermal preparation and ignition of a coal–water fuel particle was first formulated which takes into account not only the set of physical processes simultaneously occurring during the gas-phase ignition of water droplets, but also the diffusion of gaseous products of thermal decomposition of the CWF coal component in a thin layer of gas around a fuel particle. The mathematical model was verified by comparative analysis of the main integral characteristics of the ignition process (ignition delay) obtained numerically [solution of system (1)–(21)] and experimentally [14]. Comparison showed that they are in satisfactory agreement. The ignition of volatiles was found to occur at some distance (about half the CWF droplet diameter) from the fuel particle surface. Accordingly, the use of the method of reduced thin film [10] in simulating the ignition of CWF droplets is not always justified.

The predictive modeling of coke ignition shows that the initiation of combustion of the coke residue occurs almost immediately after volatile ignition. The time interval between the ignition of volatiles and coke carbon does not exceed 0.5 s. The results of the comparative analysis of the theoretical and experimental [14] time characteristics of the ignition process generally indicate that the developed mathematical model has a high predictive potential.

The results of mathematical modeling also show that the longest process in the thermal preparation of fuel to the beginning of combustion due to the high endothermic effect (up to 2.5 MJ/kg) is water evaporation.

Accordingly, for the stable ignition of CWF particles in the combustion space, it is necessary to organize zones of constant flame recycling by analogy with Shershnev combustors [35].

REFERENCES

1. J. P. Longwell, E. S. Rubin, and J. Wilson, "Coal: Energy for the Future," Prog. Energy Combust. Sci. **21** (4), 269–360 (1995).

2. B. G. Miller, "Coal–Water Slurry Fuel Utilization and Industrial Boilers," Chem. Eng. Prog. **85** (3), 29–38 (1989).

3. G. Papachristodoulou and O. Trass, "Coal Slurry Fuel Technology," Can. J. Chem. Eng. **65** (2), 177–201 (1987).

4. A. Kijo-Kleczkowska, "Combustion of Coal–Water Suspensions," Fuel **90**, 865–877 (2011).

5. W. Gajewski, A. Kijo-Kleczkowska, J. Leszczyn, "Analysis of Cyclic Combustion of Solid Fuels," Fuel **88**, 221–234 (2009).

6. R. H. Essenhigh, K. M. Mahendra, and D. W. Shaw, "Ignition of Coal Particles: A Review," Combust. Flame **77** (1), 3–30 (1989).

7. Z. Huang, et al., "Theoretical Analysis on CWM Drop Combustion History," in *Proc. 8th Int. Symp. Coal Slurry Fuels Preparation and Utilization* (USA, Orlando, 1986), Part 1, pp. 343–358.

8. K. J. Matthews and A. R. Jones, "Composition of Coal–Water Slurry Combustion and Ash Deposition Characteristics," in *Proc. 8th Int. Symp. Coal Slurry Fuels Preparation and Utilization* (USA, Orlando, 1986), Part 1, pp. 388–407.

9. V. V. Salomatov, S. V. Syrodoy, and N. Y. Gutareva, "Modelling of Heat and Mass Transfer to Solve the Problem of Particle Ignition Water–Coal Fuel," IOP Conf. Ser.: Mater. Sci. Eng. **66**, 012040 (2014).

10. G. V. Kuznetsov, V. V. Salomatov, and S. V. Syrodoy, "Numerical Simulation of Ignition of Water Coal Fuel Particles," Fiz. Goreniya Vzryva **51** (4), 12–19 (2015) [Combust., Expl., Shock Waves **51** (4), 409–415 (2015)].

11. G. V. Kuznetsov, V. V. Salomatov, and S. V. Syrodoi, "The Influence of Heat Transfer Conditions on the Parameters Characterizing the Ignition of Coal–Water Fuel Particles," Teploenergetika, No. 10, 16–21 (2015) [Thermal Eng., No. 10, 703–707 (2015)].

12. S. V. Syrodoi, G. V. Kuznetsov, and V. V. Salomatov, "Effect of the Shape of Particles on the Characteristics of the Ignition of Coal–Water Fuel," Khim. Tv. Topliva, No. 6, 28–34 (2015) [Solid Fuel Chem., No. 6, 365–371 (2015)].

13. S. V. Syrodoi, V. V. Salomatov, and G. V. Kuznetsov, "Heat and Mass Transfer in a Coal–Water Fuel Particle at the Stage of 'Thermal' Treatment," Teplofiz. Aeromekh. **23** (4), 627–636 (2016) [Thermophys. Aeromech. **23** (4), 603–612 (2016)].

14. S. V. Syrodoi, G. V. Kuznetsov, A. V. Zhakharevicha, N. Y. Gutareva, and V. V. Salomatov, "The Influence of the Structure Heterogeneity on the Characteristics and Conditions of Coal–Water Fuel Particles Ignition in High Temperature Environment," Combust. Flame **80**, 196–206 (2017).

15. D. A. Frank-Kamenetskii, *Diffusion and Heat Transfer in Chemical Kinetics* (Izd. Akad. Nauk SSSR, Moscow, 1947; Plenum, New York, 1969).

16. D. B. Spalding, *Some Fundamentals of Combustion* (Academic Press, New York, 1955)

17. Y. A. Kook, W. B. Seung, and E. C. Chang, "Investigation of a Coal–Water Slurry Droplet Exposed to Hot Gas Stream," Combust. Sci. Technol. **97** (4), 429–447.

18. O. Knacke and I. N. Stranski, "The Mechanism of Evaporation," Prog. Metal Phys. **6**, 181–235 (1956).

19. A. V. Potapkin and D. Yu. Moskvichev, "Calculation of Shock-Wave Parameters Far from Origination by Combined Numerical-Analytical Methods," Prikl. Mekh. Tekh. Fiz. **52** (2), 15–26 (2011) [J. Appl. Mech. Tech. Phys. **52** (2), 169–177 (2011)].

20. A. A. Khashchenko, O. V. Vecher, and E. I. Diskaeva, "Temperature Dependence of the Rate of Evaporation of Liquids from the Free Surface and the Rate of Liquid Boiling on a Solid Heating Surface," Izv. Alt. Gos. Univ. **89** (1), 84–87 (2016).

21. H. Enkhzhargal and V. V. Salomatov, "Mathematical Modeling of Heat Treatment and Combustion of a Coal Particle. V. Burnout Stage," Inzh.-Fiz. Zh. **84** (4), 836–841 (2011).

22. V. I. Maksimov and T. A. Nagornova, "Influence of Heatsink from Upper Boundary on Industrial Premises Thermal Conditions at Gas Infrared Emitter Operation," EPJ Web of Conf. **76**, 01006 (2014).

23. A. A. Agroskin and V. B. Gleibman, *Thermal Physics of Solid Propellants* (Nedra, Moscow, 1980) [in Russian].

24. M. P. Vukalovich, S. L. Rivkin, and A. A. Aleksandrov, *Tables of Thermophysical Properties of Water and Water Vapor* (Izd. Standartov, Moscow, 1969) [in Russian].

25. V. G. Lipovich, *Chemistry and Processing of Coal* (Khimiya, Moscow, 1988) [in Russian].

26. V. V. Pomerantsev, *Fundamentals of the Practical Theory of Combustion* (Energoatomizdat, Leningrad, 1986) [in Russian].

27. H. Watanabe, M. Ashizawa, M. Otaka, S. Hara, and A. Inumaru, "Development on Numerical Simulation Technology of Heavy Oil Gasifier," CRIEPI Report No. W01023 (Japan, 2002).

28. J. Mantzaras, "Catalytic Combustion of Syngas," Combust. Sci. Technol. **180**, 1137–1168 (2008).

29. W. C. Jian, J. Wen, S. Lu, and J. Guo, "Single-Step Chemistry Model and Transport Coefficient Model for Hydrogen Combustion," Sci. Chin. Technol. Sci. **55**, 2163–2168 (2012).

30. X. Zhang, T. Wang, J. Xu, S. Zheng, and X. Hou, "Study on Flame–Vortex Interaction in a Spark Ignition Engine Fueled with Methane/Carbon Dioxide Gases," J. Energy Inst. **91**, 133–144 (2018).

31. P. J. Roache, *Computational Fluid Dynamics* (Hermosa, Albuquerque, 1976).

32. A. A. Samarskii, "High-Order-Accuracy Schemes for a Multidimensional Heat-Conduction Equations," Zh. Vychisl. Mat. Mat. Fiz. **5** (3), 812–840 (1963).

33. A. A. Samarskii, "Locally One-Dimensional Difference Schemes on Nonuniform Grids," Zh. Vychisl. Mat. Mat. Fiz. **3** (3), 431–466 (1963).

34. A. A. Samarskii and B. D. Moiseenko, "Cost-Effective Shock-Capturing Scheme for the Multidimensional Stefan Problem," Zh. Vychisl. Mat. Mat. Fiz. **5** (5), 816–827 (1965).

35. A. A. Shershnev, *Pneumatic Combustors* (Gosenergoizdat, Leningrad–Moscow, 1949) [in Russian].